Hamiltonian Simulation with Random Inputs

Qi Zhao,[1,2] You Zhou,[3,4] Alexander F. Shaw,[1] Tongyang Li,[5,6,7] and Andrew M. Childs[1,8,*]

[1]*Joint Center for Quantum Information and Computer Science, University of Maryland, College Park, Maryland 20742, USA*
[2]*QICI Quantum Information and Computation Initiative, Department of Computer Science, The University of Hong Kong, Pokfulam Road, Hong Kong*
[3]*Key Laboratory for Information Science of Electromagnetic Waves (Ministry of Education), Fudan University, Shanghai 200433, China*
[4]*Nanyang Quantum Hub, School of Physical and Mathematical Sciences, Nanyang Technological University, 637371, Singapore*
[5]*Center on Frontiers of Computing Studies, Peking University, Beijing 100871, China*
[6]*School of Computer Science, Peking University, Beijing 100871, China*
[7]*Center for Theoretical Physics, Massachusetts Institute of Technology, Cambridge, Massachusetts 02139, USA*
[8]*Department of Computer Science and Institute for Advanced Computer Studies, University of Maryland, College Park, Maryland 20742, USA*

(Received 16 November 2021; revised 1 November 2022; accepted 21 November 2022; published 30 December 2022)

The algorithmic error of digital quantum simulations is usually explored in terms of the spectral norm distance between the actual and ideal evolution operators. In practice, this worst-case error analysis may be unnecessarily pessimistic. To address this, we develop a theory of average-case performance of Hamiltonian simulation with random initial states. We relate the average-case error to the Frobenius norm of the multiplicative error and give upper bounds for the product formula (PF) and truncated Taylor series methods. As applications, we estimate average-case error for the digital Hamiltonian simulation of general lattice Hamiltonians and k-local Hamiltonians. In particular, for the nearest-neighbor Heisenberg chain with n spins, the error is quadratically reduced from $\mathcal{O}(n)$ in the worst case to $\mathcal{O}(\sqrt{n})$ on average for both the PF method and the Taylor series method. Numerical evidence suggests that this theory accurately characterizes the average error for concrete models. We also apply our results to error analysis in the simulation of quantum scrambling.

DOI: 10.1103/PhysRevLett.129.270502

Simulating the time evolution of quantum systems is one of the most promising applications of quantum computers [1]. Quantum simulation allows quantum computers to efficiently mimic quantum dynamics, a task that is believed to be classically intractable. Quantum simulation could be applied to study numerous systems, including spin models [2], fermionic lattice models [3], quantum chemistry [4–6], and quantum field theories [7].

Following the first concrete digital quantum simulation algorithm proposed by Lloyd [8], many improved algorithms have been developed [9–13]. Algorithms are now known that have optimal or nearly optimal gate complexity with respect to several key parameters [12–16]. However, since outperforming classical computers requires controlling many qubits with high accuracy, it is challenging to realize digital quantum simulation on current hardware.

In particular, consider a Hamiltonian of the form $H = \sum_{l=1}^{L} H_l$, $\|H_l\| \leq 1$. Most known algorithms have algorithmic error scaling at least linearly with the number of terms L, making simulations of large systems costly or inaccurate [11–13,17,18]. Typical error analysis quantifies error in terms of the spectral norm, which characterizes the worst-case input and output in a Hamiltonian simulation problem. However, such an error bound can be pessimistic in practice, especially given prior knowledge of input states or measurements. In particular, error bounds can be tightened if the initial state is in a low-energy subspace [19], within the η-electron manifold [20], for measurements of local observables [21,22], and for simulations of unbounded time-dependent Hamiltonians [23].

Alternatively, to go beyond worst-case analysis and advance our theoretical understanding of quantum simulation, it is natural to quantify the performance in terms of the average error for instances drawn at random from some ensemble. In this Letter, we study such average-case performance of Hamiltonian simulation algorithms. While mathematically one can consider states drawn from the Haar measure, our analysis only requires the much weaker 1-design property, i.e., indistinguishability from the Haar measure given a single copy of the state. Note that many easily prepared sets of states form 1-designs. For instance, a locally random state $\otimes_{i=1}^{n} U_i|0\rangle^{\otimes n}$, with each U_i being a single-qubit Haar-random unitary, forms a 1-design. The uniform distribution over any orthonormal basis, such as the computational basis ensemble $\mathcal{E} = \{(1/2^n, |0\ldots00\rangle), (1/2^n, |0\ldots01\rangle), \ldots, (1/2^n, |1\ldots11\rangle)\}$,

also gives a 1-design. These inputs are widely used in quantum computing and quantum simulation tasks, so this is an average over a reasonable set of states. In general, we relate the average performance to the Frobenius norm of the multiplicative error. Intuitively, whereas worst-case error bounds scale with the largest eigenvalue of the multiplicative error, the Frobenius norm captures the *average* (specifically, root mean square) eigenvalue.

We upper bound the average error for both the pth-order product formula (PFp) method and the truncated Taylor series method [11]. For PFp, we give a bound in terms of the sum of the Frobenius norms of the $(p+1)$-layer nested commutators. In particular, we give bounds for PF1 and PF2 with detailed prefactors. Similarly to the worst-case analysis [24], for the average case we also observe destructive error interference in a nearest-neighbor Hamiltonian with the PF1 method, further tightening the error bound. In particular, we show that for a one-dimensional nearest-neighbor Heisenberg Hamiltonian with n spins, for both the PF and Taylor series methods, average-case analysis gives error $\mathcal{O}(\sqrt{n})$, quadratically smaller than the worse-case error of $\mathcal{O}(n)$.

We also explore the simulation of general k-local Hamiltonians and power-law Hamiltonians. Numerical results suggest that our analytical bounds are not far from tight in typical examples. Moreover, our techniques can be directly used to tighten the Trotter error and reduce the gate complexity in studying out-of-time-order correlators in scrambling physics. We hope that our techniques can inspire further improvements to the analytical performance of quantum simulation algorithms by leveraging particular features of specific simulations.

Worst- and average-case error.—Quantum simulation aims to realize the time-evolution operator $U_0(t) \coloneqq e^{-iHt}$ of a given Hamiltonian H. This task is crucial for studying both dynamic and static properties. In most previous methods, the distance between the ideal evolution $U_0(t)$ and the approximated evolution $U(t)$ (as implemented by some Hamiltonian simulation algorithm) is quantified by the spectral (i.e., operator) norm $\|\cdot\|$, which is the largest singular value. This measure captures the error for the worst-case input state, since

$$W(U,U_0) \coloneqq \|U-U_0\| = \max_{|\psi\rangle} \|U|\psi\rangle - U_0|\psi\rangle\|_2, \quad (1)$$

where $\|\cdot\|_2$ denotes the ℓ_2 (i.e., Euclidean) norm.

However, the worst-case error may be a significant overestimate for some initial states [23]. Instead, we consider the typical error for input states chosen at random from some ensemble $\mathcal{E} = \{(p_i, \psi_i)\}$, defined as

$$R(U,U_0) \coloneqq \mathbb{E}_{\mathcal{E}}[\mathcal{D}(U|\psi\rangle, U_0|\psi\rangle)], \quad (2)$$

where $\mathcal{D}$ is a distance measure (which we take to be either the ℓ_2 norm or the trace norm). Specifically, we study the average error and its variance, and relate them to the Frobenius norm $\|X\|_F \coloneqq \sqrt{\mathrm{Tr}(XX^\dagger)}$ (also known as the Hilbert-Schmidt norm).

For concreteness, consider the ℓ_2 norm. Using the Cauchy-Schwartz inequality, we have the upper bound $R(U,U_0) \le (\mathbb{E}_\psi \|U|\psi\rangle - U_0|\psi\rangle\|_2^2)^{1/2}$ for the average ℓ_2 error. We define the variable inside the square root as

$$S(\psi) \coloneqq \|U|\psi\rangle - U_0|\psi\rangle\|_2^2 = 2 - \langle\psi|U^\dagger U_0 + U_0^\dagger U|\psi\rangle \quad (3)$$

and calculate its expectation and variance as follows.

Theorem 1. For an input state drawn randomly from a 1-design ensemble $\mathcal{E}$ in an n-qubit Hilbert space with dimension $d \coloneqq 2^n$, the average ℓ_2 error between the ideal evolution U_0 and its approximation U has the upper bound

$$R(U,U_0) \le [\mathbb{E}_\psi S(\psi)]^{\frac{1}{2}} = \frac{1}{\sqrt{d}} \|\mathcal{M}\|_F, \quad (4)$$

where $\mathcal{M}$ is the multiplicative error, i.e., $U = U_0(\mathbb{I}+\mathcal{M})$. When the input ensemble is a 2-design, the variance of $S(\psi)$ has the upper bound $\mathrm{Var}[S(\psi)] \le [4\|\mathcal{M}\|_F^2/d(d+1)]$.

Armed with the mean and variance, we know that for an input state ψ drawn from $\mathcal{E}$, the squared error $S(\psi)$ is far from the mean value $\mathbb{E}_\psi S(\psi)$ with small probability due to the Chebyshev inequality.

This theorem can also be extended to the case where the input state is chosen at random from a subsystem of an n-qubit Hilbert space. Specifically, we have the upper bound $R^\Pi(U,U_0) \le \|\mathcal{M}\Pi\|_F/\sqrt{d_1}$, where Π projects onto a subsystem of dimension d_1. These subsystem results can be used to analyze the Trotter error in out-of-time-order correlator (OTOC) problems, as discussed in the Application section. More generally, in Section I of the Supplemental Material [25] we give results for the trace norm, approximate 1-design ensembles, and the average error with random inputs and random projections.

Average error in Hamiltonian simulation algorithms.—Two major classes of digital Hamiltonian simulation algorithms include product formula (PF) simulations and methods using linear combinations of unitaries (LCU) to directly implement the Taylor series [11]. Here we focus on the average error in PFp and Taylor series methods.

For a short evolution time t, the PF1 algorithm for a Hamiltonian $\sum_{l=1}^L H_l$ applies the unitary operation

$$\mathcal{U}_1(t) \coloneqq e^{-iH_1 t} e^{-iH_2 t} \cdots e^{-iH_L t} = \overrightarrow{\prod_l} e^{-iH_l t}. \quad (5)$$

Here the right arrow indicates the product is in the order of increasing indices. Similarly, we write $\overleftarrow{\prod}_l$ to denote a product in decreasing order. Suzuki's high-order product formulas are defined recursively by

$$\mathcal{U}_2(t) \coloneqq \overrightarrow{\prod_l} e^{-iH_l t/2} \overleftarrow{\prod_l} e^{-iH_l t/2},$$
$$\mathcal{U}_{2k}(t) \coloneqq [\mathcal{U}_{2k-2}(p_k t)]^2 \mathcal{U}_{2k-2}[(1-4p_k)t][\mathcal{U}_{2k-2}(p_k t)]^2, \quad (6)$$

where $p_k := [1/(4-4^{1/(2k-1)})]$ for $k > 1$ [36]. Overall, with $S = 2 \cdot 5^{k-1}$ stages, the evolution has the form

$$\mathcal{U}_{2k}(t) = \prod_{s=1}^{S} \prod_{l=1}^{L} e^{-ita_s H_{\pi_s(l)}}. \tag{7}$$

In each stage s, we implement evolution according to the terms in increasing or decreasing index order (specified by π_s, which is either trivial or the reversal) for time ta_s. For a long time t, we divide the evolution into r steps and apply the given product formula r times, approximating the evolution as $\mathcal{U}_{2k}^r(t/r)$. By upper bounding $\|\mathcal{M}\|_F$, we find the following bound on the average-case performance of PFp, where $p = 1$ or $p = 2k$.

Theorem 2. For the PFp simulation $\mathcal{U}_p^r(t/r)$ specified by Eq. (7), the average error in the ℓ_2 norm for a one-design input ensemble has the asymptotic upper bound $R \le \|\mathcal{M}\|_F/\sqrt{d} = \mathcal{O}(T_p t^{p+1}/r^p)$, where

$$T_p := \sum_{l_1,\ldots,l_{p+1}=1}^{L} \frac{1}{\sqrt{d}} \|[H_{l_1}, [H_{l_2}, \ldots, [H_{l_p}, H_{l_{p+1}}]]]\|_F. \tag{8}$$

Therefore $r = \mathcal{O}(T_p^{(1/p)} t^{1+(1/p)} \varepsilon^{-(1/p)})$ segments suffice to ensure average error at most ε. Furthermore, the same bounds hold for the average error with respect to the trace norm.

For comparison, the worst-case spectral norm error [18] is $W[\mathcal{U}_p^r(t/r), U_0(t)] = \mathcal{O}(\alpha_{\mathrm{comm},p} t^{p+1}/r^p)$, where

$$\alpha_{\mathrm{comm},p} := \sum_{l_1,\ldots,l_{p+1}=1}^{L} \|[H_{l_1}, [H_{l_2}, \ldots, [H_{l_p}, H_{l_{p+1}}]]]\|. \tag{9}$$

Observe that $T_p \le \alpha_{\mathrm{comm},p}$, and $\alpha_{\mathrm{comm},p}$ can be much larger than T_p. For instance, for an n-qubit nearest-neighbor Hamiltonian, $\alpha_{\mathrm{comm},p} = \mathcal{O}(n)$ and $T_p = \mathcal{O}(\sqrt{n})$. Thus we obtain a quadratic improvement with respect to the parameter n over the worst-case error scaling. For other types of Hamiltonians, we also obtain various degrees of asymptotic improvement, as shown in the Applications section.

In the following, for PF1 and PF2 we tighten the upper bounds on $\|\mathcal{M}\|_F$ by moving some summations inside the Frobenius norm and giving concrete prefactors.

Theorem 3 (Triangle bound). For the PF1 and PF2 algorithms, the average error in the ℓ_2 norm has the upper bounds

$$R[\mathcal{U}_1^r(t/r), U_0(t)] \le \frac{t^2}{r} T_1', \qquad R[\mathcal{U}_2^r(t/r), U_0(t)] \le \frac{t^3}{r^2} T_2',$$

where

$$T_1' := \frac{1}{2\sqrt{d}} \sum_{l_1=1}^{L-1} \left\| \left[H_{l_1}, \sum_{l_2=l_1+1}^{L} H_{l_2} \right] \right\|_F, \tag{10}$$

$$T_2' := \frac{1}{12\sqrt{d}} \sum_{l_1=1}^{L} \left\| \left[\sum_{l_2=l_1+1}^{L} H_{l_2}, \left[\sum_{l_2=l_1+1}^{L} H_{l_2}, H_{l_1} \right] \right] \right\|_F + \frac{1}{24\sqrt{d}} \sum_{l_1=1}^{L} \left\| \left[H_{l_1}, \left[H_{l_1}, \sum_{l_2=l_1+1}^{L} H_{l_2} \right] \right] \right\|_F. \tag{11}$$

The numerical results shown in Fig. 1 suggest that these tighter bounds can be close to optimal for PF2. However, we find a gap between the triangle bounds (green curve) and empirical results (blue curve) for PF1 with a nearest-neighbor Hamiltonian. This phenomenon results from destructive error interference between different segments that is not captured when applying the triangle inequality,

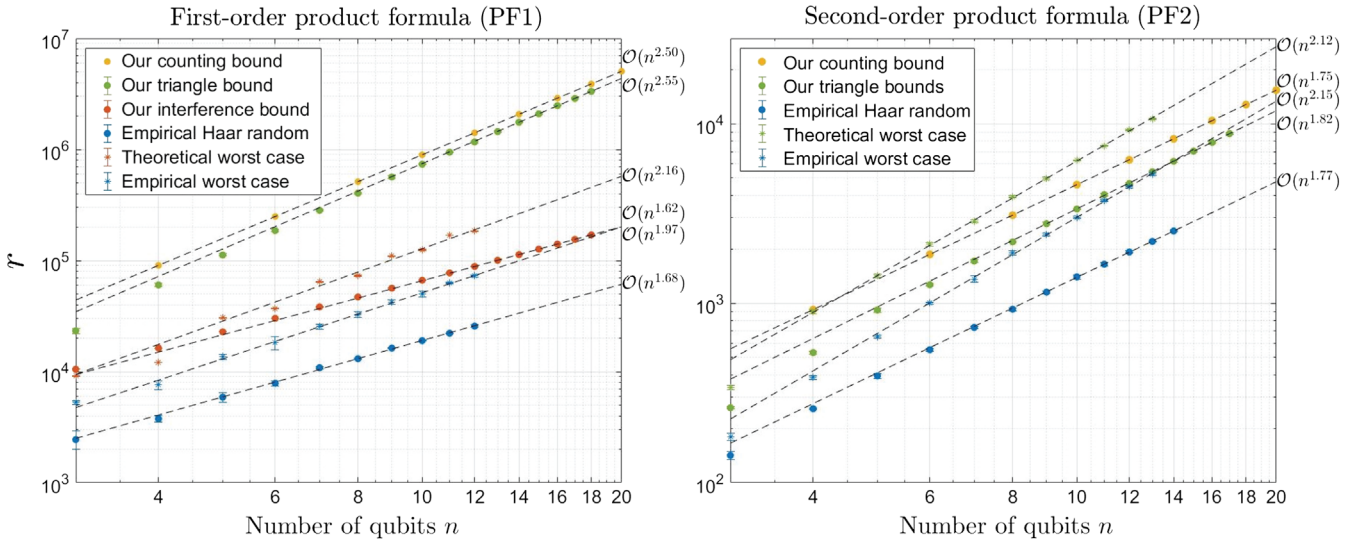

FIG. 1. Comparison of minimum r using different error bounds for the one-dimensional Heisenberg model in Eq. (15). For each system size, we generate five Hamiltonians H_i with random coefficients. We plot the mean and standard deviation of $r(t, \varepsilon, H_i)$ defined in Eq. (14).

as also seen in a previous worst-case analysis [24]. Here we further tighten the result for PF1 as follows.

Theorem 4 (Interference bound). Consider the Hamiltonian $H = \sum_{j,j+1} H_{j,j+1}$ where $H_{j,j+1}$ acts nontrivially on qubits j, $j+1$, and $\|H_{j,j+1}\| \le 1$. Let $U(t) := (e^{-iAt/r}e^{-iBt/r})^r$ where $A := \sum_{\text{odd}\,j} H_{j,j+1}$, $B := \sum_{\text{even}\,j} H_{j,j+1}$. If $\|[A,B]\|t^2/2r$ is at most a constant smaller than 1, the average error of PF1 is

$$R[U(t), U_0(t)] = \mathcal{O}\left(\sqrt{n}\left(\frac{t}{r} + \frac{t^3}{r^2}\right)\right). \tag{12}$$

This refined error analysis better reflects the empirical results (see Fig. 1). We explain this in more detail in the Supplemental Material [25].

Finally, we can also bound the average error in the Kth-order truncated Taylor series method, reducing the worst-case error $\mathcal{O}(\alpha t[(\ln 2)^{K+1}/(K+1)!])$ to $\mathcal{O}(\max_i\sqrt{\alpha_i}\alpha t[(\ln 2)^{K+1}/(K+1)!])$ where $H = \sum_{l=1}^{L}\alpha_l H_l$ and $\alpha := \sum_{i=1}^{L}\alpha_i$. However, since the gate complexity of the LCU method is logarithmic in $1/\varepsilon$, the gate reduction for the Taylor series method is mild.

Application 1: Lattice Hamiltonians.—For a lattice Hamiltonian with nearest-neighbor interactions, we have $T_p = \mathcal{O}(\sqrt{n})$ for the pth-order Trotter algorithm ($p \ge 1$). For comparison, the corresponding worst-case parameter is $\alpha_{\text{comm},p} = \mathcal{O}(n)$. Consequently, the asymptotic gate complexity is reduced from $\mathcal{O}(n^2t^2)$ in the worst case to $\mathcal{O}(n^{1.5}t^2)$ on average for PF1 (triangle bound), and from $\mathcal{O}(n^{1.5}t^{1.5})$ in the worst case to $\mathcal{O}(n^{1.25}t^{1.5})$ on average for PF2. These theoretical bounds for PF methods agree well with the empirical results shown in Fig. 1.

Application 2: k-local Hamiltonians.—Consider a k-local Hamiltonian $H = \sum_{l_1,\ldots,l_k} H_{l_1,\ldots,l_k}$ acting on n qubits, where each $H_{l_1,\ldots,l_k}$ acts nontrivially on at most k qubits. We show that the average error is related to the sum of Frobenius norms $\|H\|_{1,F} := \sum_{l_1,\ldots,l_k}\|H_{l_1,\ldots,l_k}\|_F$, an induced permutation norm $|||H|||_{\text{per}}$ defined in the Supplemental Material [25], and the induced 1-norm $|||H|||_1$ defined in Ref. [18]. Specifically, we find $T_1' = \mathcal{O}(\|H\|_{1,F}|||H|||_{\text{per}}/\sqrt{d})$ and $T_2' = \mathcal{O}(\|H\|_{1,F}|||H|||_1 \times |||H|||_{\text{per}}/\sqrt{d})$. For comparison, the commutator bounds in the worst case are $\alpha_{\text{comm},1} = \mathcal{O}(\|H\|_1|||H|||_1)$ and $\alpha_{\text{comm},2} = \mathcal{O}(\|H\|_1|||H|||_1^2)$. For simplicity, consider the case where $\|H_{l_1,\ldots,l_k}\| \le 1$ for each term. Then $\|H\|_1 \le n^k$, $\|H\|_{1,F}/\sqrt{d} \le n^k$, $|||H|||_{\text{per}} = \mathcal{O}(n^{[(k-1)/2]})$, and $|||H|||_1 = \mathcal{O}(n^{k-1})$. We summarize the resulting errors for the PF1 and PF2 in Table I. These results also apply to k-local fermionic Hamiltonians such as SYK models, as discussed in Section VI.C of the Supplemental Material [25].

Application 3: Power-law interactions.—Consider power-law interactions on a D-dimensional lattice $\Lambda \subset \mathbb{R}^D$, with two-site interactions $H = \sum_{i,j\in\Lambda} H_{i,j}$. Suppose the interaction strength decays as the power law

$$\|H_{i,j}\| \le \begin{cases} 1 & i = j \\ \frac{1}{\|i-j\|^\alpha} & i \ne j \end{cases} \tag{13}$$

for some $\alpha \ge 0$, where $\|i-j\|$ denotes the Euclidean distance. We show in the Supplemental Material [25] that $|||H|||_{\text{per}}^2 \le |||H|||_1$. We present the error scaling for power-law interactions with $0 \le \alpha < D$, $\alpha = D$, and $\alpha > D$ in Table II. The comparison to empirical performance shown in Fig. 2 suggests that our theoretical bounds are reasonably tight.

TABLE I. Errors for k-local Hamiltonian simulation with PF1 and PF2 methods.

Order	Worst-case error [18]	Average error
$p = 1$	$\mathcal{O}((t^2/r)n^{2k-1})$	$\mathcal{O}((t^2/r)n^{[(3k-1)/2]})$
$p = 2$	$\mathcal{O}((t^3/r^2)n^{3k-2})$	$\mathcal{O}((t^3/r^2)n^{[(5k-3)/2]})$

Application 4: Out-of-time-order correlators.—As a final example, consider the (infinite-temperature) OTOC for two commuting local observables X and Y, $\langle O(t)\rangle := \langle Y^\dagger(t)X^\dagger Y(t)X\rangle$ where $Y(t) := e^{iHt}Ye^{-iHt}$ in the Heisenberg picture [37,38]. To measure the OTOC in an experiment [39], an initial state $\rho \otimes I_{d_1}/d_1$ is prepared where ρ is the state of the first qubit and I_{d_1}/d_1 is the maximally mixed state of the remaining $n-1$ qubits, where $d_1 := 2^{n-1}$. After the unitary evolution $V_0 := e^{iHt}Ye^{-iHt}$ (assuming Y is unitary), the measurement X is performed on the first qubit. In practice, e^{iHt} and e^{-iHt} can be approximated via PF methods. Viewing the initial state $\rho \otimes I_{d_1}/d_1$ as a mixture of randomly chosen states on an $(n-1)$-qubit subsystem, we can use our results to quantify the Trotter error. For example, suppose H is a nearest-neighbor Hamiltonian (as described above) and e^{iHt} and e^{-iHt} are approximated via PF2. Then for a given constant Trotter error ε, we can reduce the gate complexity of an OTOC measurement from $\mathcal{O}(n^{1.5}t^{1.5})$ with worst-case analysis to $\mathcal{O}(n^{1.25}t^{1.5})$. Similar techniques can be adopted to quantify the Trotter error in algorithms to estimate $\text{Tr}(e^{-iHt})$, with applications such as the trace estimation in the one clean qubit model [40,41]. See Section VI.E of the Supplemental Material [25] for further details.

Numerical results.—To investigate the tightness of our theoretical bounds, we compare them with empirical error data. We measure the complexity in terms of the *average Trotter number* for the pth-order formula $\mathcal{U}_p$ for a given instance of Hamiltonian H_i,

$$r(t,\varepsilon,H_i) := \min\left\{r : \mathbb{E}_\psi\left\|\left(\mathcal{U}_p^r\left(\frac{t}{r}\right) - e^{-itH_i}\right)|\psi\rangle\right\|_2 \le \varepsilon\right\} \tag{14}$$

TABLE II. Errors for PF1 and PF2 simulations of power-law interaction Hamiltonians.

	$0 \le \alpha < D$		$\alpha = D$		$\alpha > D$	
Order	Worst-case error	Average error	Worst-case error	Average error	Worst-case error	Average error
$p = 1$	$\mathcal{O}((t^2/r)n^{3-2\alpha/D})$	$\mathcal{O}((t^2/r)n^{\frac{5}{2}-3\alpha/2D})$	$\mathcal{O}((t^2/r)n\log^2(n))$	$\mathcal{O}((t^2/r)n\log^{\frac{3}{2}}(n))$	$\mathcal{O}((t^2/r)n)$	$\mathcal{O}((t^2/r)n)$
$p = 2$	$\mathcal{O}((t^3/r^2)n^{4-3\alpha/D})$	$\mathcal{O}((t^3/r^2)n^{\frac{7}{2}-5\alpha/2D})$	$\mathcal{O}((t^3/r^2)n\log^3(n))$	$\mathcal{O}((t^3/r^2)n\log^{\frac{5}{2}}(n))$	$\mathcal{O}((t^3/r^2)n)$	$\mathcal{O}((t^3/r^2)n)$

which guarantees the expectation value of the error is below a given simulation accuracy ε. For each instance of H_i, we set evolution time $t = n$, error threshold $\epsilon = 10^{-3}$, and generate 20 Haar-random inputs. For comparison, we also show the worst-case empirical Trotter numbers by directly computing the spectral norm error (see the data indicated by asterisks in Figs. 1 and 2.)

Here the triangle and interference bounds correspond to the results in Theorems 3 and 4, respectively. The counting bound is presented in Sec. VII.A.3 and Sec. VII.B.2 of the Supplemental Material [25].

We first consider the one-dimensional Heisenberg model with a random magnetic field,

$$H = \sum_{j=1}^{n-1}(X_jX_{j+1} + Y_jY_{j+1} + Z_jZ_{j+1}) + \sum_{j=1}^{n} h_jZ_j, \quad (15)$$

with uniformly random coefficients $h_j \in [-1, 1]$. The Hamiltonian summands can be partitioned into two sets in an even-odd pattern [42]. Figure 1 compares the empirical Trotter number for PF1 and PF2 with the theoretical bounds in Theorems 3 and 4. The interference bound curve and the triangle bound curve match the empirical results for PF1 and PF2 well, respectively. However, because of the additional assumption of Theorem 4, for large t and n, $\mathcal{O}(nt^2/r)$ will dominate, significantly increasing r. The analysis in the worst case also suffers from a similar problem [24]. We elaborate on this point in the Supplemental Material [25]. The techniques in Ref. [43] may help to strengthen and simplify our interference bound.

We also consider the one-dimensional Heisenberg model with power-law interactions, with the Hamiltonian

$$\sum_{j=1}^{n-1}\sum_{k=j+1}^{n}\frac{1}{|j-k|^\alpha}(X_jX_k + Y_jY_k + Z_jZ_k) + \sum_{j=1}^{n} h_jZ_j \quad (16)$$

with uniformly randomly coefficients $h_j \in [-1, 1]$ and α a parameter controlling the decay of the interactions. We consider a rapidly decaying power law with $\alpha = 4$ and the infinite-range case with $\alpha = 0$. We analyze product formulas with X-Y-Z order [17], as shown in Fig. 2. We again find that our error bounds are reasonably tight in many cases, but are somewhat loose for PF1 with shorter-range interactions. In particular, for the $\alpha = 0$ case, extrapolation suggests an improvement by 2 orders of magnitude at $n = 50$. For more detail, see Table IV of the Supplemental Material [25].

In Section VII of the Supplemental Material [25], we also show empirical results for PF4 and PF6 (which align well with our asymptotic results in Theorem 2), other

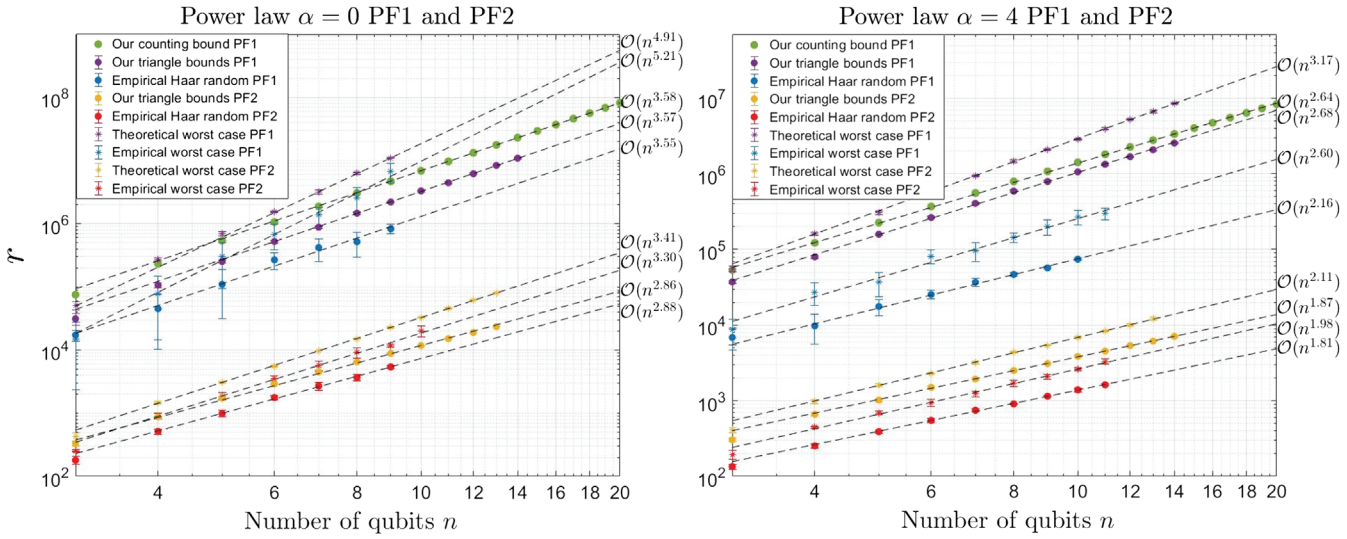

FIG. 2. Comparison of minimum r using different error bounds for the one-dimensional Heisenberg model with power-law interactions in Eq. (16).

1-design inputs, and the standard deviations of random inputs.

Conclusions and open problems.—In this Letter, we have developed a theory of average error for Hamiltonian simulation with random input states. Though previous methods already provide optimal performance in terms of worst-case error, we find further improvement when considering the average case. Our techniques might also be extended to quantify the algorithmic error in imaginary time evolution [44] and quantum Monte Carlo methods [45,46]. Moreover, the average error performance could be achieved by entangled states whose local density matrices are (approximately) maximally mixed, such as the k-uniform state [47], suggesting a connection between the simulation algorithm error and quantum thermalization.

We are grateful to Jiaqi Leng and Xiaodi Wu for their useful discussions. We also thank Jiaqi Leng for assistance with our numerical results. After completing this work, we became aware of related work by [48] that also analyzes Trotter errors with random input states. Q. Z. and A. F. S. acknowledge the support of the Department of Defense through the QuICS Hartree Postdoctoral Fellowship and Lanczos Graduate Fellowship, respectively. Q. Z. acknowledges the support from HKU Seed Fund for New Staff. Y. Z. acknowledges the support of NSFC No. 12205048, the Singapore MOE Tier 1 Grant No. RG162/19 and RG146/20, and FQXi-RFP-IPW-1903. T. L. was supported by the NSF Grant No. PHY-1818914 and a Samsung Advanced Institute of Technology Global Research Partnership. A. M. C. received support from the National Science Foundation (Grant No. CCF-1813814 and QLCI Grant No. OMA-2120757) and the Department of Energy, Office of Science, Office of Advanced Scientific Computing Research, Quantum Algorithms Teams and Accelerated Research in Quantum Computing programs.

*Corresponding author.
amchilds@umd.edu

[1] R. P. Feynman, Int. J. Theor. Phys. **21**, 467 (1982).
[2] R. Somma, G. Ortiz, J. E. Gubernatis, E. Knill, and R. Laflamme, Phys. Rev. A **65**, 042323 (2002).
[3] D. Wecker, M. B. Hastings, N. Wiebe, B. K. Clark, C. Nayak, and M. Troyer, Phys. Rev. A **92**, 062318 (2015).
[4] D. Wecker, B. Bauer, B. K. Clark, M. B. Hastings, and M. Troyer, Phys. Rev. A **90**, 022305 (2014).
[5] R. Babbush, J. McClean, D. Wecker, A. Aspuru-Guzik, and N. Wiebe, Phys. Rev. A **91**, 022311 (2015).
[6] R. Babbush, P. J. Love, and A. Aspuru-Guzik, Sci. Rep. **4**, 6603 (2014).
[7] S. P. Jordan, K. S. Lee, and J. Preskill, Science **336**, 1130 (2012).
[8] S. Lloyd, Science **273**, 1073 (1996).
[9] D. W. Berry, G. Ahokas, R. Cleve, and B. C. Sanders, Commun. Math. Phys. **270**, 359 (2007).
[10] D. W. Berry and A. M. Childs, Quantum Inf. Comput. **12**, 29 (2012).
[11] D. W. Berry, A. M. Childs, R. Cleve, R. Kothari, and R. D. Somma, Phys. Rev. Lett. **114**, 090502 (2015).
[12] G. H. Low and I. L. Chuang, Phys. Rev. Lett. **118**, 010501 (2017).
[13] G. H. Low and I. L. Chuang, Quantum **3**, 163 (2019).
[14] D. W. Berry, A. M. Childs, and R. Kothari, in *56th Annual IEEE Symposium on Foundations of Computer Science* (IEEE, New York, 2015), pp. 792–809.
[15] A. M. Childs and Y. Su, Phys. Rev. Lett. **123**, 050503 (2019).
[16] G. H. Low, in *Proceedings of the 51st Annual ACM Symposium on Theory of Computing* (Association for Computing Machinery, New York, 2019), pp. 491–502.
[17] A. M. Childs, D. Maslov, Y. Nam, N. J. Ross, and Y. Su, Proc. Natl. Acad. Sci. U.S.A. **115**, 9456 (2018).
[18] A. M. Childs, Y. Su, M. C. Tran, N. Wiebe, and S. Zhu, Phys. Rev. X **11**, 011020 (2021).
[19] B. Şahinoğlu and R. D. Somma, npj Quantum Inf. **7**, 119 (2021).
[20] Y. Su, H.-Y. Huang, and E. T. Campbell, Quantum **5**, 495 (2021).
[21] M. Heyl, P. Hauke, and P. Zoller, Sci. Adv. **5**, eaau8342 (2019).
[22] C.-F. Chen, H.-Y. Huang, R. Kueng, and J. A. Tropp, PRX Quantum **2**, 040305 (2021).
[23] D. An, D. Fang, and L. Lin, Quantum **5**, 459 (2021).
[24] M. C. Tran, S.-K. Chu, Y. Su, A. M. Childs, and A. V. Gorshkov, Phys. Rev. Lett. **124**, 220502 (2020).
[25] See Supplemental Material at http://link.aps.org/supplemental/10.1103/PhysRevLett.129.270502 for theoretical and numerical details, which includs Refs. [25–35].
[26] R. A. Low, arXiv:1006.5227.
[27] H. Zhu, R. Kueng, M. Grassl, and D. Gross, arXiv:1609.08172.
[28] A. W. Harrow, arXiv:quant-ph/1308.6595.
[29] Z. Webb, Quantum Inf. Comput. **16**, 1379 (2016).
[30] H. Zhu, Phys. Rev. A **96**, 062336 (2017).
[31] K. R. W. Jones, J. Phys. A **24**, 1237 (1991).
[32] A. Kitaev, A Simple Model of Quantum Holography (2015), https://online.kitp.ucsb.edu/online/entangled15/kitaev/.
[33] S. Sachdev and J. Ye, Phys. Rev. Lett. **70**, 3339 (1993).
[34] S. Xu, L. Susskind, Y. Su, and B. Swingle, arXiv:2008.02303.
[35] P. Jordan and E. Wigner, Z. Phys. **47**, 631 (1928).
[36] M. Suzuki, J. Math. Phys. (N.Y.) **32**, 400 (1991).
[37] S. H. Shenker and D. Stanford, J. High Energy Phys. 03 (2014) 001.
[38] J. Maldacena, S. H. Shenker, and D. Stanford, J. High Energy Phys. 08 (2016) 001.
[39] J. Li, R. Fan, H. Wang, B. Ye, B. Zeng, H. Zhai, X. Peng, and J. Du, Phys. Rev. X **7**, 031011 (2017).
[40] E. Knill and R. Laflamme, Phys. Rev. Lett. **81**, 5672 (1998).
[41] C. Cade and A. Montanaro, in *Proceedings of the 13th Conference on the Theory of Quantum Computation, Communication and Cryptography (TQC 2018)*, Leibniz International Proceedings in Informatics (LIPIcs) Vol. 111, edited by S. Jeffery (Schloss Dagstuhl–Leibniz-Zentrum fuer Informatik, Dagstuhl, Germany, 2018), pp. 4:1–4:20.
[42] A. M. Childs and Y. Su, Phys. Rev. Lett. **123**, 050503 (2019).

[43] D. Layden, Phys. Rev. Lett. **128**, 210501 (2022).
[44] M. Motta, C. Sun, A. T. Tan, M. J. O'Rourke, E. Ye, A. J. Minnich, F. G. Brandão, and G. K.-L. Chan, Nat. Phys. **16**, 205 (2020).
[45] S. Bravyi, Quantum Inf. Comput. **15**, 1122 (2015).
[46] S. Bravyi and D. Gosset, Phys. Rev. Lett. **119**, 100503 (2017).
[47] A. J. Scott, Phys. Rev. A **69**, 052330 (2004).
[48] C.-F. Chen and F. G. S. L. Brandão, arXiv:2111.05324.